Plant Stress 14 (2024) 100668

Contents lists available at ScienceDirect

Plant Stress

journal homepage: www.sciencedirect.com/journal/plant-stress

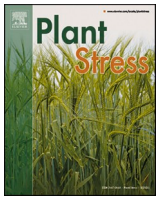

Histochemical and gene expression changes in *Cannabis sativa* hypocotyls exposed to increasing concentrations of cadmium and zinc

Roberto Berni [a], Jean-Francois Hausman [a], Stanley Lutts [b], Gea Guerriero [a,*]

[a] Environmental Research and Innovation Department, Luxembourg Institute of Science and Technology, 5, rue Bommel, l-4940, Hautcharage, Luxembourg
[b] Groupe de Recherche en Physiologie Végétale (GRPV), Earth and Life Institute–Agronomy (ELI-A), Université Catholique de Louvain, Croix du Sud 45, boîte L7.07.13, B-1348, Louvain-la-Neuve, Belgium

ARTICLE INFO

Keywords:
Textile hemp
Bast fibres
Cadmium
Zinc
Cell wall

ABSTRACT

Hemp (*Cannabis sativa* L.) is a versatile crop that produces cellulosic bast fibres used in textiles and biocomposites. Is also finds use in phytoremediation, being a good candidate for the cultivation on marginal lands, such as those contaminated by heavy metals (HMs). HMs like cadmium (Cd) and zinc (Zn) are known to affect plant growth and impair the biosynthesis of cellulose and lignin at the cell wall level. Since cellulose is the major component in the gelatinous layer of bast fibres, HMs can impact the structure of hemp fibres and, consequently, their mechanical properties. This study investigates how varying concentrations of Cd and Zn in the soil affect the bast fibres of hemp plantlets. The chosen model is the hypocotyl, as it is ideal for studying bast fibre development: it exhibits a temporal separation between the elongation and thickening phases within a short period of approximately three weeks. *C. sativa* plantlets were grown for 20 days, and the hypocotyls sampled to perform histochemical observations, gene expression analysis, as well as to quantify biomass yield and Cd/Zn accumulation. Hemp plantlets grown in soils with the three highest Zn concentrations were smaller than the control group, whereas no decrease in size was observed under elevated Cd concentrations. However, at the highest Cd concentration, the root system exhibited enhanced development, accompanied by a significant increase in dry weight across all the concentrations tested. The quantification of Cd and Zn showed that the roots were the main organs accumulating HMs. Cd at the two highest concentrations decreased significantly the lumen area of bast fibres and increased their cell wall thickness. Zn decreased significantly the lumen area, but it did not impact the thickness of the cell wall at the highest concentration. Cd also increased the number of secondary fibres. Immunohistochemistry highlighted a different pattern of crystalline cellulose distribution with a signal that was less homogeneous in the presence of Cd and Zn. Gene expression analysis revealed changes in transcripts encoding cellulose synthases, fasciclin-like arabinogalactan proteins, class III peroxidases. The results obtained shed light on the molecular response and bast fibre histological changes occurring in young hemp plants exposed to Cd and Zn.

1. Introduction

Soil contamination by heavy metals (HMs) causes significant environmental and public health concerns. These contaminants primarily originate from industrial activities, agricultural practices, such as the application of low quality fertilisers and plant protection products (Luyckx et al., 2021a), and urbanisation (Zhu et al., 2024). Contamination by HMs leads to the degradation of soil quality with consequent risks to human health, ecosystems, and food safety.

Cadmium (Cd) is a highly toxic HM, and its presence in soil is concerning because it is highly mobile, especially at low pH, and it can be taken up by plants via metal transporters or non-selective cation channels (Huang et al., 2020), thereby entering the food chain and posing a threat to health (Wang et al., 2023).

While zinc (Zn) is indispensable in small amounts for plant growth and human health (Sharma et al., 2013), it can become toxic at elevated levels (Hussain et al., 2022). High concentrations of Zn can not only inhibit plant growth, but also alter the rhizomicrobiome (Guarino et al., 2020) and impact the soil microbial activity (Liu et al., 2020).

The persistence and mobility of these elements in the soil exacerbate their impact, making remediation efforts challenging and costly.

Soil remediation can be achieved via several techniques, either *ex-*

* Corresponding author.
E-mail address: gea.guerriero@list.lu (G. Guerriero).

https://doi.org/10.1016/j.stress.2024.100668
Received 26 August 2024; Received in revised form 18 October 2024; Accepted 7 November 2024
Available online 8 November 2024

situ or *in-situ* (Liu et al., 2018), each suited to different contamination scenarios and soil physico-chemical conditions. The former can achieve higher levels of contaminant removal compared to *in-situ* techniques, but are costlier and more disruptive as they imply excavating the contaminated soil from the affected area, transporting it to a secure waste disposal site or treatment facility, and disposing of it at approved locations (Liu et al., 2018).

Among *in-situ* techniques, phytoremediation is a sustainable method leveraging natural processes, as it relies on plants that extract/immobilise/stabilise HMs. This technique presents several benefits, namely preservation of soil integrity and of ecosystem's biodiversity. Studies have indeed shown that phytoremediation can improve soil structure, increase organic matter, and enhance microbial activity, leading to healthier soils post-remediation (Nkongolo et al., 2022). The performance of phytoremediation can be improved when coupled to other methods, such as physical, chemical (i.e., addition of chelating agents) and microbiological ones (Kalousek et al., 2024; Tan et al., 2023). Last but not least, the use of plants improves the aesthetic value of a contaminated site, transforming it into a green space, thus contributing to ecological restoration (Islam et al., 2024).

The biomass produced on contaminated soils can be valorised as a source of biopolymers, or biofuel which creates revenues, thereby adhering to the principles of bio-economy (Ionata et al., 2024). However, correct post-treatment of the contaminated biomass is needed to avoid the incidence of secondary pollution and to provide cost-effective and environmental-safe methods converting the biomass into useful byproducts (Liu and Tran, 2021).

Industrial hemp (*Cannabis sativa* L.) has emerged as a promising candidate for phytoremediation because of its remarkable capacity to uptake HMs (Golia et al., 2023; Guo et al., 2024; Luyckx et al., 2021a). Its rapid growth and extensive root system not only facilitate the stabilisation and decontamination of polluted sites, but also improve soil structure. This last feature makes it an excellent break crop (Finnan and Styles, 2013).

Studies investigating the cultivation of hemp on marginal lands showed higher levels of HMs in roots than stems and leaves, a finding that justifies the prospective valorisation of the above-ground tissues of this crop. As a matter of fact, a study demonstrated that fibres obtained from stems of *C. sativa* growing on Pb- (lead), Cd- and Zn-contaminated soils met the safety standards for textile use (De Vos et al., 2022), while another reported the presence of higher concentrations of cannabidiol and the absence of detectable levels of Cu (copper) in flowers of hemp growing on Cu-contaminated soils (Vasilou et al., 2024). Research carried out on hemp (cv. Futura 75) grown on contaminated sites (with Pb, Cd and Zn) in Northern France also indicated that shivs and fibres could be used for applications such as insulating material and concrete agglomerates (i.e., biomaterials that do not set the HMs free), or also to produce energy in thermal power plants with regulated combustion methods (Luyckx et al., 2022).

The cell walls of bast fibres are rich in crystalline cellulose and lignin-poor, characteristics that contribute to their remarkable tensile and mechanical properties (Andre et al., 2016; Manaia et al., 2019; Mokshina et al., 2018). They are multi-layered, with a thicker gelatinous cell wall predominantly composed of cellulose microfibrils aligned parallel to the fibre axis. This structural alignment provides high tensile strength and stiffness.

The presence of HMs affects cell wall biosynthesis which can, in turn, influence the overall mechanical properties of bast fibres (Luyckx et al., 2022). Emblematic is the alteration of pectin metabolism whereby modifications in the esterification level can determine the capacity of the cell wall to bind HMs like Cd (reviewed in Parrotta et al., 2015).

The hemp hypocotyl was shown to be a suitable model to address questions related to cell wall biogenesis in bast fibres as it shows a well-defined temporal separation between elongation and thickening (Behr et al., 2016, 2018a, 2018b).

The present study aims at elucidating the histochemical modifications and the changes in expression of cell wall-related genes in the hemp hypocotyl grown on soils with increasing concentrations of Cd and Zn. The goal is to complement and enrich the results previously published on hemp grown in hydroponics in the presence of HMs (Luyckx et al., 2021a).

2. Materials and methods

2.1. Soil preparation and sampling of plant tissues

Seeds of *Cannabis sativa* (monoecious var. Santhica 27) were purchased from the agricultural cooperative HEMPit (https://www.hemp-it.coop/en/) and grown on potting soil (obtained by mixing 1/3 sand and 2/3 peat moss) with vermiculite (1 kg mixed with 7 kg of soil) containing different concentration of $CdCl_2$ (1.8, 4.6, 11.4, 28.5 mg/kg) and $ZnCl_2$ (13.7, 20.4, 30.7, 46 mg/kg). $CdCl_2$ and $ZnCl_2$ were dissolved in 2 l of water and mixed with the soil using a concrete mixer. The soil was left to dry on a table overnight after spreading it; the concrete mixer was thoroughly washed between the treatments and left to dry overnight prior to re-use. Seeds were sown in a top layer of uncontaminated potting soil (ca. 1.5 cm) and put in controlled growth chambers set at 60 % relative humidity and with a cycle of 16 h light at 25 °C/8 h dark at 20 °C. Plants were watered twice a week by adding 100 ml tap water to each pot. Three biological replicates composed by 3 plants each were prepared per condition, and harvested at 6, 12, 20 days after sowing. Leaves, hypocotyls (segment excised immediately below the cotyledons and above the radicle) and epicotyls (stem segment above the cotyledons) were excised, ground to a fine powder and either stored at −80 °C or lyophilised for subsequent elemental analysis. Roots were also sampled by taking care to retrieve them as intact as possible from the soil; they were extensively washed and blotted dry on paper tissues. For fresh weight (FW) determination, tissues were immediately weighed; for dry weight (DW) determination, the tissues were weighed after lyophilisation which lasted 72h.

2.2. Sample preparation for microscopy

The procedure to prepare the hypocotyl samples for immunohistochemistry followed the steps described previously (Behr et al., 2016). The observation of the CBM3a signal was performed with a fluorescence microscope (Olympus BX43). FASGA staining followed the procedure described in Tolivia and Tolivia (1987). The lumen area of the fibres and the cell wall thickness were calculated with the ImageJ 1.53k software.

2.3. Gene expression analysis with qPCR

The extraction of RNA, the assessment of purity and integrity, as well as the preparation of cDNA and qPCR were done as described earlier (Behr et al., 2016). The primers used were reported in previous studies (Behr et al., 2018b; Guerriero et al., 2017a, 2017b). The reference genes *F-box* and *CDPK* were used for normalisation (Mangeot-Peter et al., 2016).

2.4. ICP-MS analysis

The lyophilised ground leaves, roots, epicotyls were mineralised in a microwave oven Multiwave Pro (Anton Paar) as described in Guerriero et al. (2021). After mineralisation, the final volume was brought to 25 ml with ultra-pure water, then the samples were centrifuged at 4700 rpm for 10 min, filtered through 0.2 μm filters and analysed with an ICP-MS (7900 ICP-MS, Agilent). The quantifications were performed with a calibration curve from 0.25 to 2500 μg/l for ^{66}Zn and from 0.025 to 250 μg/L for ^{111}Cd. Blanks and quality control standards were analysed every ten samples. ^{103}Rh and ^{185}Re were used as internal standards to correct for any factor impacting the analyte signals. After measurement, the dilution and the recovery factors obtained from the certified

reference material (*Citrus* leaves, NCS ZC 73,018, LGC Standards) were applied to the mineralised samples. The concentrations were then expressed in μg of element per g of lyophilised sample.

2.5. Statistics

Data were $\log_{10}$-transformed before performing statistics with IBM SPSS statistics v19. Normality was assessed using the Shapiro-Wilk test; homogeneity was checked with the Levene's test. For normal and homogeneous data, a one-way ANOVA with Tukey's post hoc text was carried out; for those not following normal distribution and/or not homogeneous, a Kruskal-Wallis test was performed with Dunn's post hoc test.

3. Results and discussion

3.1. Impact of Cd and Zn on biomass yield and accumulation in hemp tissues

Under Cd exposure, changes in FW and DW were observed for the epicotyls and roots, while no significant differences were present in the leaves (Fig. 1). Plants exposed to Cd showed an increase in epicotyl FW which was significant at 4.6 mg/kg Cd (Fig. 1a); the differences were however not significant for the dry biomass (Fig. 1b). In roots exposed to 4.6 and 11.4 mg/kg Cd, significant higher fresh biomass values were observed (Fig. 1a); the DW was significantly higher (corresponding to an increase of +68 %, +155 %, +147 %, +113 % compared to the control) in all the conditions tested (Fig. 1b). Under higher Zn concentrations, significant changes were observed: at 30.7 mg/kg Zn, higher values of FW were observed for leaves, epicotyls and roots compared to the control (Fig. 1c). Significant higher values than the control were also observed for the DW in epicotyls at 30.7 and 46 mg/kg Zn (corresponding to an increase of +112 % and +91 % compared to the control) and roots at 30.7 mg/kg Zn (corresponding to an increase of +92 % compared to the control) (Fig. 1d).

While at the two highest Cd concentration no significant differences were noticed for the stem length, an increase was observed at the root level after 20 days of exposure (Supplementary Fig. 1a). Hemp plantlets grown in the presence of the highest Zn concentration showed a decrease in the stem length and no significant changes at the root level

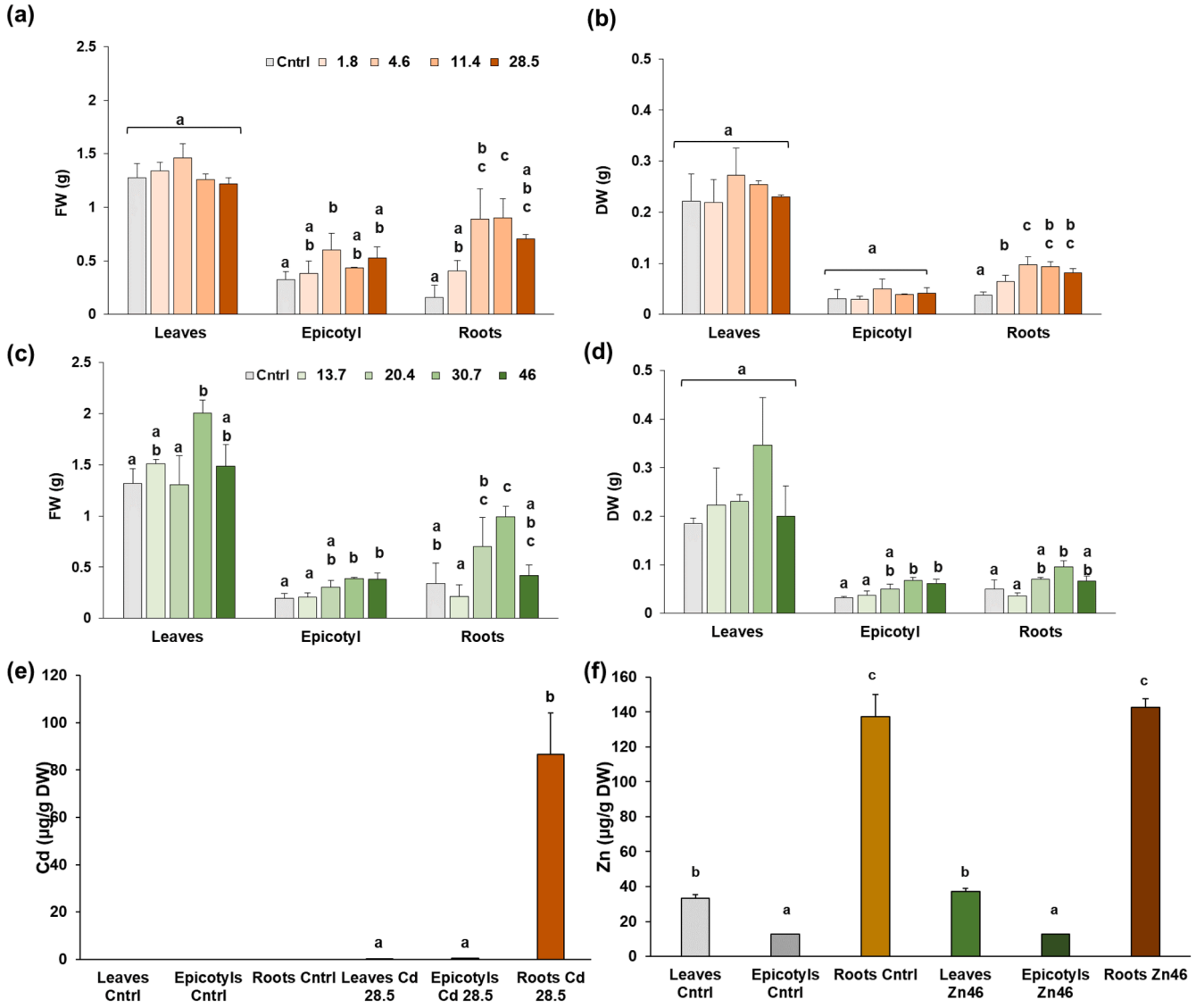

Fig. 1. FW, DW, Cd and Zn concentration in *C. sativa* leaves, epicotyls, and roots exposed or not to Cd and Zn. (a, b), 20 days-old plants exposed to increasing concentrations of Cd (in mg/kg); (c, d), 20 days-old plants exposed to increasing concentrations of Zn (in mg/kg); (e), Cd concentrations (in μg/g DW of tissues) in organs of plantlets exposed to 28.5 mg/kg Cd; (f), Zn concentration (in μg/g DW of tissues) in organs of plantlets exposed to 46 mg/kg Zn. Error bars indicate the standard deviation ($n = 3$). Different letters indicate statistically different values among groups ($p < 0.05$).

(Supplementary Fig. 1b).

Cd (20 μM) was previously shown to impact root biomass in 4 weeks-old hemp plants grown in hydroponics: a 53 % decrease in biomass was indeed reported, which was accompanied by an increase in phytochelatins, as well as in the expression of a proline biosynthetic gene and the abundance of transcripts coding for heat shock proteins (Luyckx et al., 2021b). In the present study, a significant increase in the root dry biomass was observed at 1.8, 11.4 and 28.5 m/kg Cd. The roots are the organs in which Cd accumulates at the highest level in hemp (Luyckx et al., 2021a, 2021b) and cell walls are known to be able to sequester Cd (Parrotta et al., 2015). An increase in root biomass during the early stages of hemp growth may provide a higher occurrence of Cd adsorption sites (either through cell wall polysaccharides such as cellulose, pectins, aliphatic-aromatic barrier such as suberin and/or proteins). However, this remains at this stage a hypothesis and further studies will be needed on older hemp plants to verify whether other mechanisms, such as stiffening of the cell walls may occur with consequent growth arrest phenotype at the root level.

The cultivation modalities of this study compared to the previous ones (soil-grown vs hydroponics), different Cd concentrations and exposure time (20 days vs 1 week) can also account for the differences observed in terms of root biomass. In a hydroponic system, Cd is more readily available to the plants because it is dissolved directly in the nutrient solution; this high availability leads to rapid Cd uptake and accumulation in the roots, causing immediate toxic effects. In contrast, HMs may bind to soil particles and their bioavailability may consequently be quite lower than in nutrient solution. Although sand particles used in our substrate are not expected to retain HM cations, peat commonly exhibits a high density of negative charges which could strongly bind Cd^{2+} or Zn^{2+} ions (Zhu et al., 2023). Additionally, the direct exposure to Cd in hydroponics induces significant stress responses in plants, such as the production of reactive oxygen species (ROS) and activation of cell rescue mechanisms at both the gene- and protein-levels (Luyckx et al., 2021b). These stress responses may divert energy and resources away from growth, leading to a reduced root biomass.

Cd accumulated at the highest level in roots, followed by epicotyls and leaves (Fig. 1e); Zn was also found at the highest level in roots, followed by leaves and epicotyls (Fig. 1f). These results confirm previous findings reporting hemp roots as organs accumulating high levels of HMs (Flajšman et al., 2023; Golia et al., 2023; Luyckx et al., 2021a).

3.2. Histological impact of Cd and Zn on hemp hypocotyls

A time-course histochemical analysis was performed on hemp hypocotyls exposed to Cd and sampled at 6–12–20 days after sowing (Fig. 2). The differences among Cd treatments were not evident at 6d: the cortical parenchyma occupied most of the tissue cross-sections and the primary xylem composed of the bigger metaxylem and smaller protoxylem was visible with the FASGA coloration at the two poles around the pith (Fig. 2 top row). The metaxylem was more developed at 4.6 mg/kg, forming a ring around the pith.

At 12d, primary bast fibres were present (Fig. 2 middle row, arrows), while at 20d, both primary and secondary fibres (dashed arrows) were well visible (Fig. 2 bottom row).

A stimulatory effect of Cd at the highest concentration was observed in hypocotyls aged 20 days: a broader layer of secondary fibres was indeed present (Fig. 3 top row, double ended arrows). Under exposure to the two highest Cd concentrations, the cell walls of primary bast fibres were also thicker compared to the control condition, and the lumen area was smaller (Supplementary Fig. 2a and b).

Similar results were previously observed in 10 days-old flax hypocotyls exposed to Cd 0.5 mM: an acceleration of bast fibres' differentiation was described, together with thicker cell walls, a response mechanism providing an increased amount of uronic acids sequestering Cd (Douchiche et al., 2011).

The distribution of cellulose was subsequently studied using the His-tagged recombinant cellulose binding module CBM3a (Blake et al., 2006). Differences in cellulose distribution and in signal intensity were noticed (Fig. 3 bottom row). While under control condition a uniform signal was present across the bast fibre gelatinous layer (G-layer), it became scattered, as well as less intense and homogeneous, with *punctae* that were particularly evident at the highest concentration. The intensity of the signal also decreased at higher Cd concentrations, a finding suggesting alterations in the cellulose phases (decrease of the crystalline phase or increase in the amorphous phase) under Cd exposure.

At 6 days, the cross section of hypocotyls exposed to the highest concentration of Zn showed a more developed metaxylem extending around the central pith, differently from the other conditions where the metaxylem was localised at the two poles around the pith (Fig. 4 top row). At 12 days, primary bast fibres were present (Fig. 4 middle row), and at 20 days secondary bast fibres were also well visible (Fig. 4 bottom

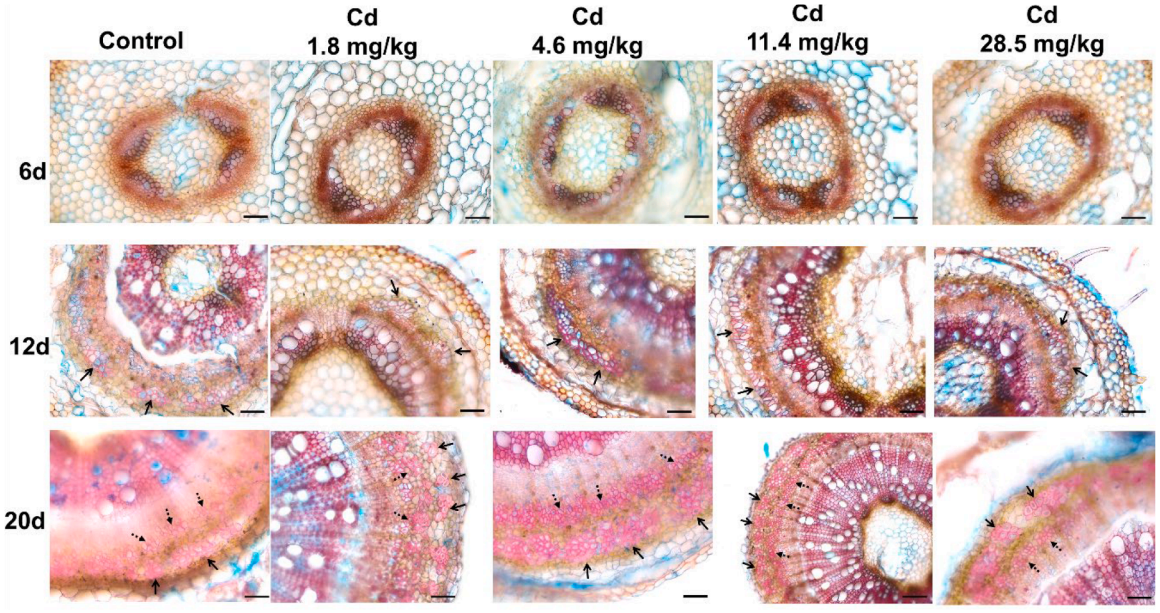

Fig. 2. Panel showing the hypocotyl sections at 6–12–20 days and at the different Cd concentrations observed with FASGA coloration. Arrows point to primary bast fibres, dashed arrows to secondary fibres. Scale bars indicate 50 μm.

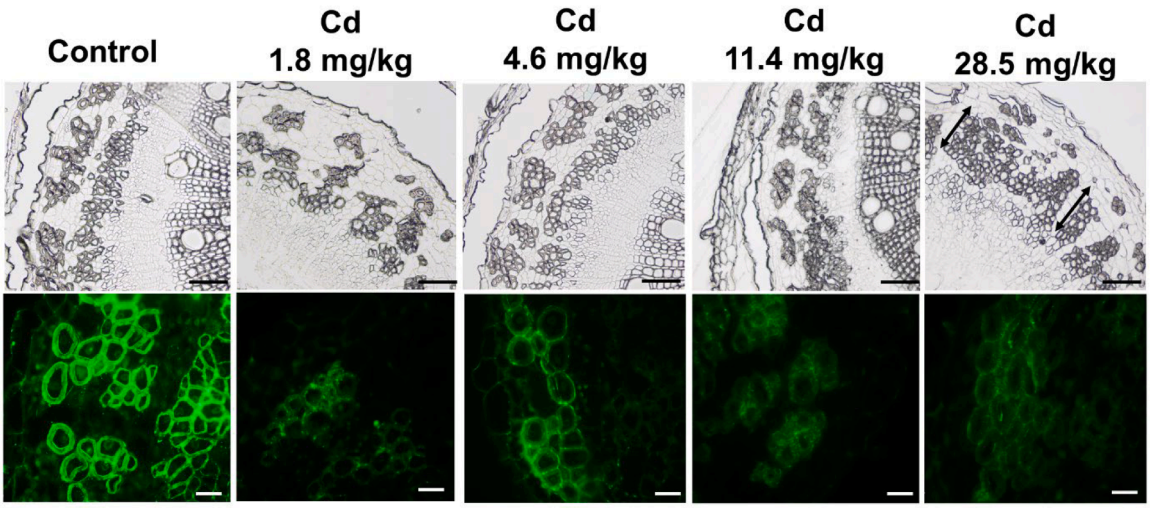

Fig. 3. Panel showing the hypocotyl sections at 20 days and at the different Cd concentrations observed in brightfield (top row) and after incubation with the fluorescent protein-tagged CBM3a (bottom row). The double ended arrows point to the layer of secondary fibres. Scale bars indicate 50 μm in the top panels and 20 μm in the bottom panels.

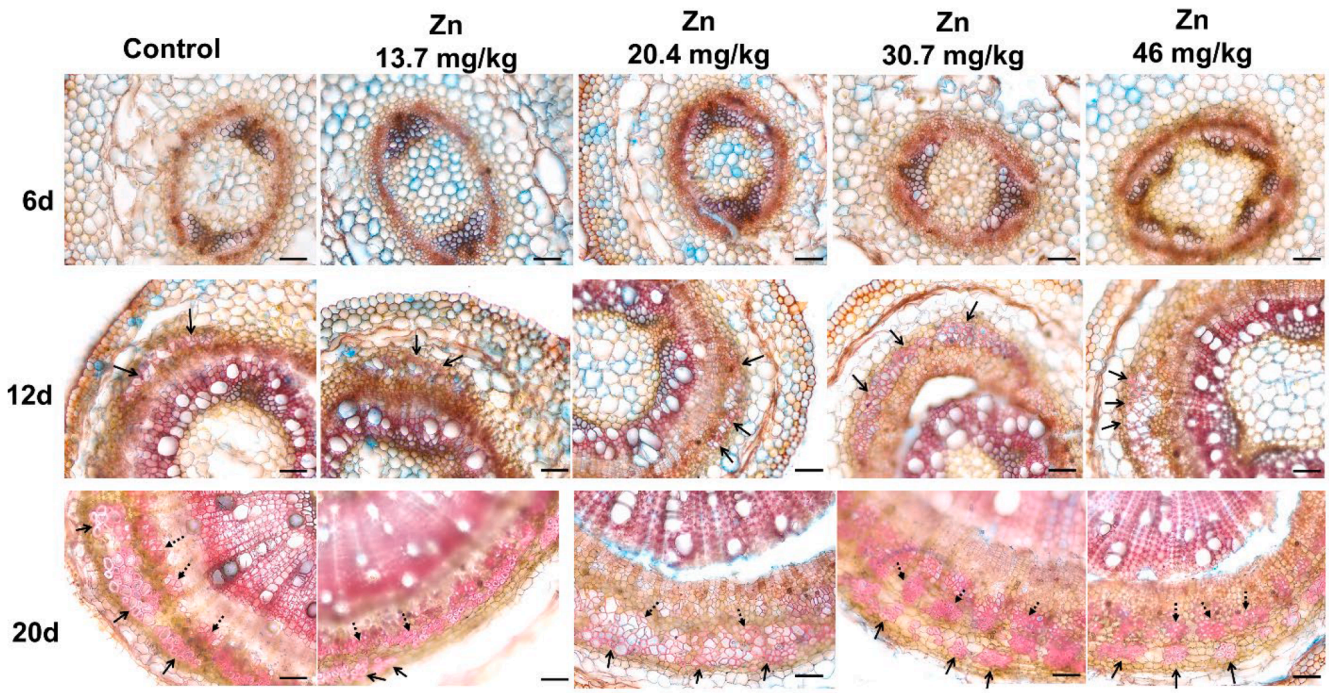

Fig. 4. Panel showing the hypocotyl sections at 6–12–20 days and at the different Zn concentrations observed with FASGA coloration. Arrows point to primary bast fibres, dashed arrows to secondary fibres. Scale bars indicate 50 μm.

row, dashed arrows).

Differently from Cd, the highest Zn concentration did not cause any significant increase in the thickness of primary bast fibres' cell walls (Supplementary Fig. 2c), but it caused a decrease in their lumen area (Supplementary Fig. 2d) and number (Fig. 5), as previously reported in older plants (Luyckx et al., 2021a).

Zn also promoted the development of secondary fibres at 13.7 mg/kg Zn (Fig. 5 top row, double ended arrows).

Compared to the control and similarly to what observed with Cd, the CBM3a signal was less homogeneous in the presence of Zn, where more intense areas were observed in the gelatinous cell walls, giving it a "striped" appearance (Fig. 5 bottom row).

The alterations observed in cellulose distribution can be explained by considering the link that exists between cellulose biosynthesis and the level of pectin methylesterification, a parameter determining the capacity to bind HMs. The etiolated hypocotyls of thale cress *trichome birefringence* (*tbr*) mutants were shown to have a decreased degree of pectin methylesterification, accompanied by an increased activity of pectin methylesterase (PME) and decreased cellulose levels in trichomes and stems (Bischoff et al., 2010).

The G-layer of hemp bast fibres is known to undergo extensive post-synthetic remodelling: changes in the β-(1,4)-D-galactan side chains of rhamnogalacturonan I transform a stripped Gn-layer into the solid G-layer (Chernova et al., 2018), and the fibrillar Gf-layer detected in the bast fibres of hemp plantlets undergoes compaction as the hypocotyl matures (Behr et al., 2019). Considering that the presence of

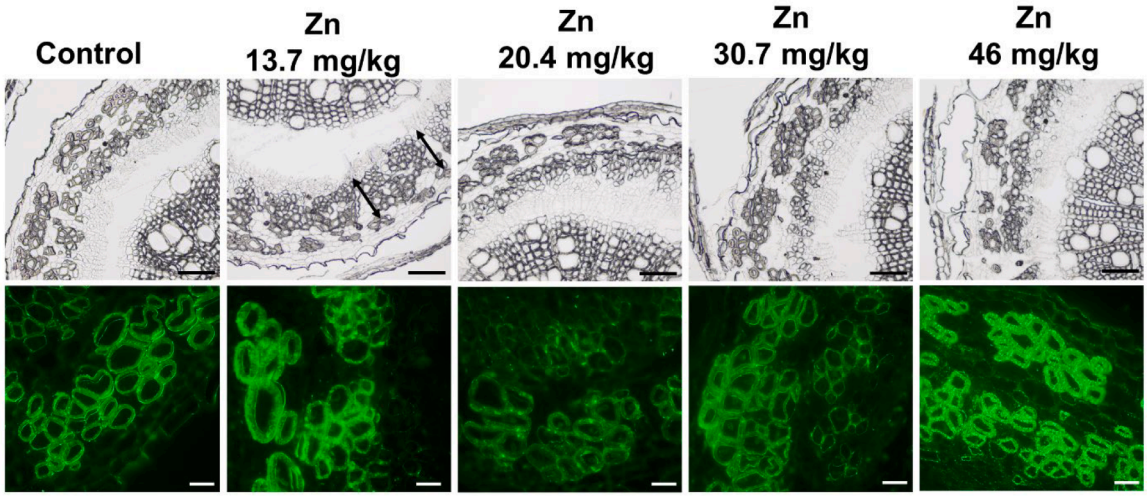

Fig. 5. Panel showing the hypocotyl sections at 20 days and at the different Zn concentrations observed in brightfield (top row) and after incubation with the fluorescent protein-tagged CBM3a (bottom row). The double ended arrows point to the layer of secondary fibres. Scale bars indicate 50 μm in the top panels and 20 μm in the bottom panels.

homogalacturonan (HG) was demonstrated in *Cannabis* bast fibres with the use of LM19 (Chernova et al., 2018), it is legitimate to suppose a connection between HG methylesterification status and cellulose deposition in hemp fibres. Alterations in pectin methylesterification (such as those triggered by Zn- and Cd-exposure) may cause modifications in the deposition of cellulose in the G-layer, similarly to what observed in the trichomes and stems of *Arabidopsis tbr* mutants. This is further supported by recent findings demonstrating that enzymatic or chemical alterations in the pectin nanopatterning determined by Ca-HG nodes result in a rearrangement of cellulose microfibrils (Siemianowski et al., 2024).

3.3. Molecular impact of Cd and Zn on cell wall-related genes

Targeted gene expression analysis was performed on hypocotyls aged 20 days grown in the presence of increasing concentrations of Cd and Zn (Fig. 6). Transcripts previously reported to vary in expression during the hypocotyl development and in response to exogenous stresses were specifically targeted (Behr et al., 2016; Berni et al., 2020, 2022). These genes code for the secondary cell wall cellulose synthases *CesA4–7–8*, fasciclin-like arabinogalactan proteins *FLA18–20–24*, the laccase *LAC11*, as well as the peroxidases *PRX49–52–72*.

Cd significantly upregulated the expression of *CesA4* at 28.5 mg/kg Cd and *CesA7* at 4.6–11.4–28.5 mg/kg; a tendency towards increased expression was noticed for *CesA4* and *CesA7* as the Cd concentrations increased to 1.8, 4.6, 11.8 and 1.8 mg/kg, respectively, but the differences were not significant compared to the control.

Zn supplementation significantly increased the expression of *CesA4* at all the concentrations studied with respect to the control. No significant changes were observed for the other cellulose synthases.

In cotton, Cd upregulated the expression of *CesA4–7–8*: stimulating cellulose deposition increases the number of hydroxyl groups capable of sequestering Cd in the apoplast (Chen et al., 2019; Šípošová et al., 2023).

An enhanced secondary cell wall biosynthesis is commonly described in plants exposed to HMs: the increased thickness accompanies stiffening which in turn explains the decreased cell wall extensibility and reduced growth observed (Wakabayashi et al., 2023). Cell wall stiffening is additionally promoted by pectin changes under HM exposure: lowering the degree of pectin methylesterification increases the number of negative charges capable of forming a pectate gel ("egg-box" model) with cations.

Thickening of the bast fibre cell walls (Suppl. Fig. 2a) could also be due to swelling caused by higher hydration compared to the control condition: as hypothesised in flax, Cd can have an impact on the enzymes responsible for the remodelling of the G-layer, or can directly disturb cellulose biosynthesis by interacting with negative charges in the plasma membrane (Douchiche et al., 2011).

Among the *FLA*s, only *FLA18* showed significant differences at 1.8, 4.6 and 28.5 mg/kg Cd. *FLA18* in hemp is orthologous to *FLA11* in thale cress (Guerriero et al., 2017b), a protein involved in secondary cell wall biogenesis and stem mechanics (MacMillan et al., 2010). The increased expression of *FLA18* follows the expression trend of secondary cell wall *CesA*s and may explain the altered distribution of the CBM3a signal observed in the G-layer of bast fibres exposed to Cd (Fig. 3). CBM3a recognises crystalline cellulose and the lack of homogeneity in its signal under Cd treatment indicates modifications in the crystallisation of cellulose mirofibrils. Such changes were previously reported in Cd-exposed flax hypocotyls (Douchiche et al., 2011). A link between arabinogalactan proteins and cellulose is known to exist (Lin et al., 2022): for example, it was suggested that FLAs and cellulose synthesis are linked via an ethylene-independent pathway involving 1-aminocyclopropane-1-carboxylate (ACC) and receptor kinases. Additionally, arabinogalactan proteins interact with cell wall components, such as pectins and hemicelluloses, which are in their turn associated with cellulose. Arabinogalactan proteins thus act as structural components affecting cellulose deposition.

Under Zn supplementation, *FLA18* decreased instead in expression, suggesting the occurrence of different cell wall-related mechanisms in the hemp hypocotyl exposed to Cd and Zn.

Among the genes coding for enzymes involved in lignification, only class III peroxidases showed significant changes in expression following Cd and Zn exposure. Notably, the expression trend of *PRX49* was opposite between Cd and Zn treatment: while it decreased at 11.4 mg/kg Cd compared to the condition with 1.8 mg/kg, it increased at all the Zn concentrations studied. *PRX52* did not show any changes under Cd treatment, while it decreased in expression at 46 mg/kg Zn. *PRX72* was downregulated at higher Cd concentrations.

The peroxidases chosen are involved in lignification and are expressed at higher levels in older hypocotyls (Behr et al., 2018b). It should however be noted that the use of an anti-PRX antibody previously revealed accumulation in the cytoplasm in younger hypocotyl aged 9 days and secretion in the cell walls at later stages with labelling of the G-layer in 20-days-old hemp hypocotyls (Behr et al., 2019). PRXs were thus suggested to play a role in the modification of the G-layer during the development of the hypocotyl and to be involved, to a lesser extent, in the development of the S1-layer. The different expression pattern observed suggests distinct roles in relation to cell wall biogenesis in the

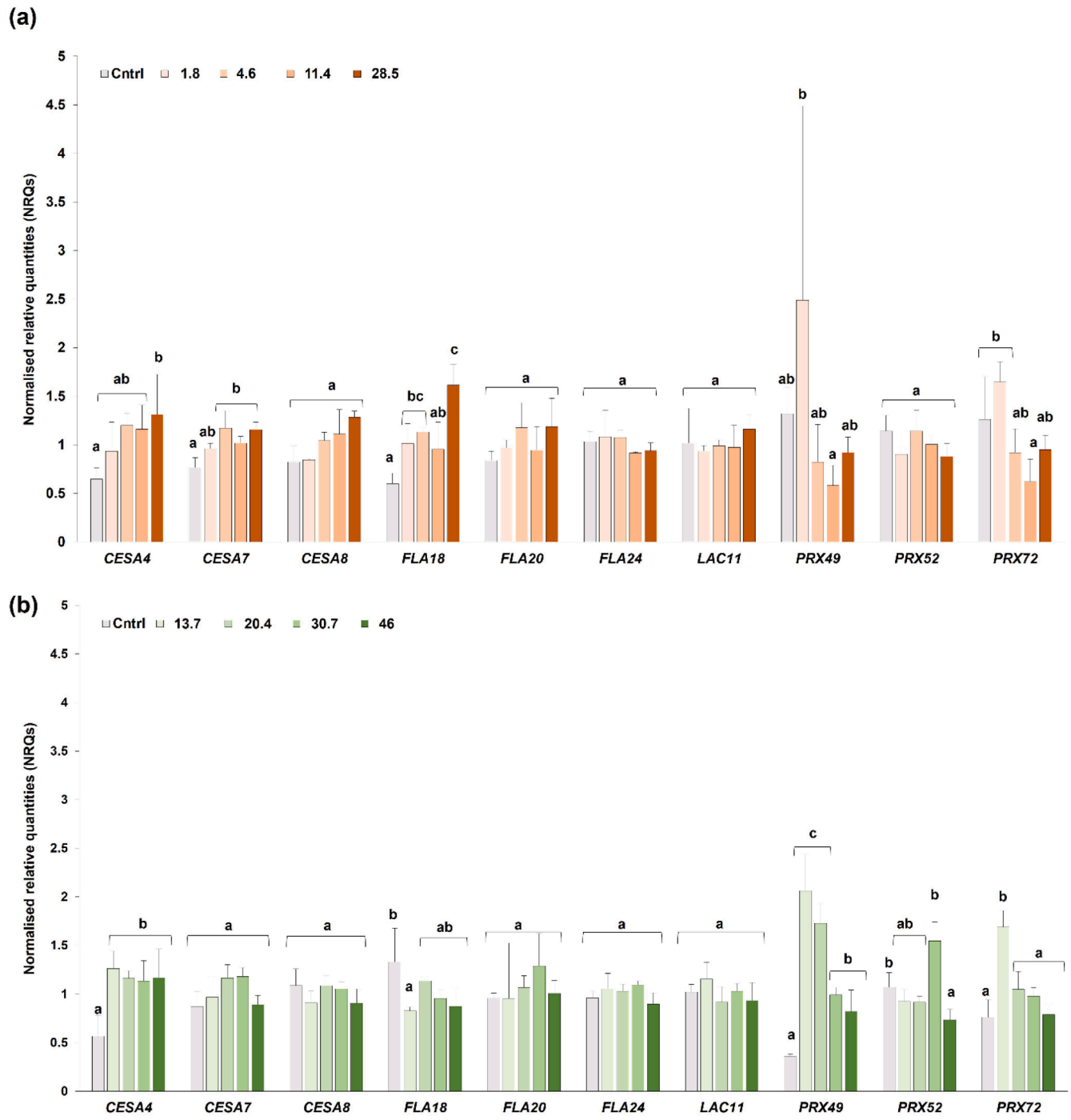

Fig. 6. Bar chart showing the qPCR results. (a), data relative to 20 days-old hypocotyls exposed to Cd (in mg/kg); (b), data relative to 20 days-old hypocotyls exposed to Zn (in mg/kg). Error bars indicate the standard deviation ($n = 3$). Different letters indicate statistically significant differences among groups ($p < 0.05$).

mature hemp hypocotyl exposed to Cd and Zn.

4. Conclusion

Hemp plantlets exposed to higher concentrations of Zn developed smaller stems compared to the control, while elevated Cd levels led to an increase in root biomass, where these elements accumulated at the highest levels. The bast fibres in the hypocotyls showed major histochemical modifications upon exposure to HMs. Cd decreased the fibre lumen area, increased the thickness of the G-layer and stimulated the development of secondary bast fibres. It also altered the distribution of crystalline cellulose, as revealed using the fluorescent protein-tagged CBM3a: the signal became less homogeneous and intense than the control, with the presence of *punctae*. Zn at the highest concentration decreased the lumen area of primary bast fibres, and it also altered the distribution of the CBM3a signal which conferred to the G-layer a striped appearance. The expression of cell wall-related genes was altered upon exposure to Cd and Zn. Two secondary cell wall *CesA*s and *FLA18* increased in expression under Cd stress, while class III peroxidases showed either a decrease or no changes. Under Zn stress, *CesA4* and *PRX49* increased in expression, while *FLA18* transcript tended to decrease in abundance. Overall, the results obtained show that exposure to Cd and Zn induces major histological alterations in hemp bast fibres and triggers a transcriptional response characterised by a common

induction of cellulose biosynthetic genes and differing expression patterns of other cell wall-related genes. A longer cultivation period than the one here studied (closer to the cultivation time typically used for hemp fibre production) would allow for a more detailed investigation into key plant biometric parameters and cell wall composition. Biometric measurements, including stem diameter, leaf area, root volume, could provide insights into the structural development of hemp organs under HM exposure. Likewise, analysing the leaf and root anatomy will provide important insights into histological response mechanisms in source and sink tissues. Additionally, cell wall analysis would be crucial in understanding the potential modifications of the fibres due to HM, shedding light on important implications for both industrial applications and environmental risk assessment.

Funding source

This research was supported by the Luxembourg National Research Fund (INTER/FNRS/20/15045745). For the purpose of open access, and in fulfilment of the obligations arising from the grant agreement, the authors have applied a Creative Commons Attribution 4.0 International (CC BY 4.0) license to any Author Accepted Manuscript version arising from this submission.

CRediT authorship contribution statement

Roberto Berni: Writing – original draft, Visualization, Validation, Software, Methodology, Investigation, Formal analysis, Data curation, Conceptualization. **Jean-Francois Hausman:** Writing – review & editing, Resources, Conceptualization. **Stanley Lutts:** Writing – review & editing, Supervision, Resources, Project administration, Methodology, Investigation, Funding acquisition, Conceptualization. **Gea Guerriero:** Writing – review & editing, Writing – original draft, Validation, Supervision, Resources, Project administration, Methodology, Investigation, Funding acquisition, Formal analysis, Data curation, Conceptualization.

Declaration of competing interest

The authors declare that they have no known competing financial interests or personal relationships that could have appeared to influence the work reported in this paper.

Acknowledgments

The authors would like to thank Laurent Solinhac for the help with the plant cultures and Dr. Kjell Sergeant for the suggestions on the experimental set-up. Dr. Denis Pittois and Dr. Cédric Guignard are also thanked for their support with the ICP-MS analyses.

Supplementary materials

Supplementary material associated with this article can be found, in the online version, at doi:10.1016/j.stress.2024.100668.

Data availability

All the data are reported in the manuscript.

References

Andre, C.M., Hausman, J.F., Guerriero, G., 2016. *Cannabis sativa*: the plant of the thousand and one molecules. Front. Plant Sci. 7, 19. https://doi.org/10.3389/fpls.2016.00019.

Behr, M., Faleri, C., Hausman, J.F., Planchon, S., Renaut, J., Cai, G., Guerriero, G., 2019. Distribution of cell-wall polysaccharides and proteins during growth of the hemp hypocotyl. Planta 250, 1539–1556. https://doi.org/10.1007/s00425-019-03245-9.

Behr, M., Legay, S., Žižková, E., Motyka, V., Dobrev, P.I., Hausman, J.F., Lutts, S., Guerriero, G., 2016. Studying secondary growth and bast fiber development: the hemp hypocotyl peeks behind the wall. Front. Plant Sci. 7, 1733. https://doi.org/10.3389/fpls.2016.01733.

Behr, M., Lutts, S., Hausman, J.F., Guerriero, G., 2018a. Jasmonic acid to boost secondary growth in hemp hypocotyl. Planta 248, 1029–1036. https://doi.org/10.1007/s00425-018-2951-5.

Behr, M., Sergeant, K., Leclercq, C.C., Planchon, S., Guignard, C., Lenouvel, A., Renaut, J., Hausman, J.F., Lutts, S., Guerriero, G., 2018b. Insights into the molecular regulation of monolignol-derived product biosynthesis in the growing hemp hypocotyl. BMC Plant Biol. 18, 1. https://doi.org/10.1186/s12870-017-1213-1.

Berni, R., Hausman, J.F., Villas-Boas, S., Guerriero, G., 2022. Impact of *Pseudomonas* sp. SVB-B33 on stress- and cell wall-related genes in roots and leaves of hemp under salinity. Horticulturae 8, 336. https://doi.org/10.3390/horticulturae8040336.

Berni, R., Mandlik, R., Hausman, J.F., Guerriero, G., 2020. Silicon-induced mitigatory effects in salt-stressed hemp leaves. Physiol. Plant 171, 476–482. https://doi.org/10.1111/ppl.13097.

Bischoff, V., Nita, S., Neumetzler, L., Schindelasch, D., Urbain, A., Eshed, R., Persson, S., Delmer, D., Scheible, W.R., 2010. *TRICHOME BIREFRINGENCE* and its homolog *AT5G01360* encode plant-specific DUF231 proteins required for cellulose biosynthesis in *Arabidopsis*. Plant Physiol. 153, 590–602. https://doi.org/10.1104/pp.110.153320.

Blake, A.W., McCartney, L., Flint, J.E., Bolam, D.N., Boraston, A.B., Gilbert, H.J., Knox, J. P., 2006. Understanding the biological rationale for the diversity of cellulose-directed carbohydrate-binding modules in prokaryotic enzymes. J. Biol. Chem. 281, 29321–29329. https://doi.org/10.1074/jbc.M605903200.

Chen, H., Li, Y., Ma, X., Guo, L., He, Y., Ren, Z., Kuang, Z., Zhang, X., Zhang, Z., 2019. Analysis of potential strategies for cadmium stress tolerance revealed by transcriptome analysis of upland cotton. Sci. Rep. 9, 86. https://doi.org/10.1038/s41598-018-36228-z.

Chernova, T.E., Mikshina, P.V., Salnikov, V.V., Ibragimova, N.N., Sautkina, O.V., Gorshkova, T.A., 2018. Development of distinct cell wall layers both in primary and secondary phloem fibers of hemp (*Cannabis sativa* L.). Ind. Crops Prod. 117, 97–109. https://doi.org/10.1016/j.indcrop.2018.02.082.

De Vos, B., Souza, M.F., Michels, E., Meers, E., 2022. Industrial hemp (*Cannabis sativa* L.) in a phytoattenuation strategy: remediation potential of a Cd, Pb and Zn contaminated soil and valorization potential of the fibers for textile production. Ind. Crops Prod. 178, 114592. https://doi.org/10.1016/j.indcrop.2022.114592.

Douchiche, O., Driouich, A., Morvan, C., 2011. Impact of cadmium on early stages of flax fibre differentiation: ultrastructural aspects and pectic features of cell walls. Plant Physiol. Biochem. 49, 592–599. https://doi.org/10.1016/j.plaphy.2011.03.008.

Finnan, J., Styles, D., 2013. Hemp: a more sustainable annual energy crop for climate and energy policy. Energy Policy 58, 152–162. https://doi.org/10.1016/j.enpol.2013.02.046.

Flajšman, M., Košmelj, K., Grčman, H., Ačko, D.K., Zupan, M., 2023. Industrial hemp (*Cannabis sativa* L.)—A valuable alternative crop for growing in agricultural soils contaminated with heavy metals. Environ. Sci. Pollut. Res. 30, 115414–115429. https://doi.org/10.1007/s11356-023-30474-z.

Golia, E.E., Bethanis, J., Ntinopoulos, N., Kaffe, G.G., Komnou, A.A., Vasilou, C., 2023. Investigating the potential of heavy metal accumulation from hemp. The use of industrial hemp (*Cannabis sativa* L.) for phytoremediation of heavily and moderated polluted soils. Sustain. Chem. Pharm. 31, 100961. https://doi.org/10.1016/j.scp.2022.100961.

Guarino, F., Improta, G., Triassi, M., Cicatelli, A., Castiglione, S., 2020. Effects of zinc pollution and compost amendment on the root microbiome of a metal tolerant poplar clone. Front. Microbiol. 11, 1677. https://doi.org/10.3389/fmicb.2020.01677.

Guerriero, G., Behr, M., Hausman, J.F., Legay, S., 2017a. Textile hemp vs. salinity: insights from a targeted gene expression analysis. Genes 8, 242. https://doi.org/10.3390/genes8100242. . (Basel).

Guerriero, G., Mangeot-Peter, L., Legay, S., Behr, M., Lutts, S., Siddiqui, K.S., Hausman, J.F., 2017b. Identification of fasciclin-like arabinogalactan proteins in textile hemp (*Cannabis sativa* L.): *in silico* analyses and gene expression patterns in different tissues. BMC Genom. 18, 741. https://doi.org/10.1186/s12864-017-3970-5.

Guerriero, G., Sutera, F.M., Torabi-Pour, N., Renaut, J., Hausman, J.F., Berni, R., Pennington, H.C., Welsh, M., Dehsorkhi, A., Zancan, L.R., Saffie-Siebert, S., 2021. Phyto-courier, a silicon particle-based nano-biostimulant: evidence from *Cannabis sativa* exposed to salinity. ACS Nano 15, 3061–3069. https://doi.org/10.1021/acsnano.0c09488.

Guo, Y., Wen, L., Zhao, X., Xing, C., Huang, R., 2024. Industrial hemp (*Cannabis sativa* L.) can utilize and remediate soil strongly contaminated with Cu, As, Cd, and Pb by phytoattenuation. Chemosphere 358, 142199. https://doi.org/10.1016/j.chemosphere.2024.142199.

Huang, X., Duan, S., Wu, Q., Yu, M., Shabala, S., 2020. Reducing cadmium accumulation in plants: structure–function relations and tissue-specific operation of transporters in the spotlight. Plants 9, 223. https://doi.org/10.3390/plants9020223. . (Basel).

Hussain, S., Khan, M., Sheikh, T.M.M., Mumtaz, M.Z., Chohan, T.A., Shamim, S., Liu, Y., 2022. Zinc essentiality, toxicity, and its bacterial bioremediation: a comprehensive insight. Front. Microbiol. 13, 900740. https://doi.org/10.3389/fmicb.2022.900740.

Ionata, E., Caputo, E., Mandrich, L., Marcolongo, L., 2024. Moving towards biofuels and high-value products through phytoremediation and biocatalytic processes. Catalysts 14, 118. https://doi.org/10.3390/catal14020118.

Islam, M.M., Saxena, N., Sharma, D., 2024. Phytoremediation as a green and sustainable prospective method for heavy metal contamination: a review. RSC Sustain. 2, 1269–1288. https://doi.org/10.1039/D3SU00440F.

Kalousek, P., Holátko, J., Schreiber, P., Pluháček, T., Širůčková Lónová, K., Radziemska, M., Tarkowski, P., Vyhnánek, T., Hammerschmiedt, T., Brtnický, M.,

2024. The effect of chelating agents on the Zn-phytoextraction potential of hemp and soil microbial activity. Chem. Biol. Technol. Agric. 11, 23. https://doi.org/10.1186/s40538-024-00544-6.

Lin, S., Miao, Y., Huang, H., Zhang, Y., Huang, L., Cao, J., 2022. Arabinogalactan proteins: focus on the role in cellulose synthesis and deposition during plant cell wall biogenesis. Int. J. Mol. Sci. 23, 6578. https://doi.org/10.3390/ijms23126578.

Liu, L., Li, W., Song, W., Guo, M., 2018. Remediation techniques for heavy metal-contaminated soils: principles and applicability. Sci. Total Environ. 633, 206–219. https://doi.org/10.1016/j.scitotenv.2018.03.161.

Liu, Y.M., Cao, W.Q., Chen, X.X., Yu, B.G., Lang, M., Chen, X.P., Zou, C.Q., 2020. The responses of soil enzyme activities, microbial biomass and microbial community structure to nine years of varied zinc application rates. Sci. Total Environ. 737, 140245. https://doi.org/10.1016/j.scitotenv.2020.140245.

Liu, Z., Tran, K.-Q., 2021. A review on disposal and utilization of phytoremediation plants containing heavy metals. Ecotoxicol. Environ. Saf. 226, 112821.

Luyckx, M., Blanquet, M., Isenborghs, A., Guerriero, G., Bidar, G., Waterlot, C., Douay, F., Lutts, S., 2022. Impact of silicon and heavy metals on hemp (*Cannabis sativa* L.) bast fibres properties: an industrial and agricultural perspective. Int. J. Environ. Res. 16, 82. https://doi.org/10.1007/s41742-022-00446-1.

Luyckx, M., Hausman, J.F., Isenborghs, A., Guerriero, G., Lutts, S., 2021a. Impact of cadmium and zinc on proteins and cell wall-related gene expression in young stems of hemp (*Cannabis sativa* L.) and influence of exogenous silicon. Environ. Exp. Bot. 183, 104363. https://doi.org/10.1016/j.envexpbot.2020.104363.

Luyckx, M., Hausman, J.F., Sergeant, K., Guerriero, G., Lutts, S., 2021b. Molecular and biochemical insights into early responses of hemp to Cd and Zn exposure and the potential effect of si on stress response. Front. Plant Sci. 12, 711853. https://doi.org/10.3389/fpls.2021.711853.

MacMillan, C.P., Mansfield, S.D., Stachurski, Z.H., Evans, R., Southerton, S.G., 2010. Fasciclin-like arabinogalactan proteins: specialization for stem biomechanics and cell wall architecture in *Arabidopsis* and *Eucalyptus*. Plant J. 62, 689–703. https://doi.org/10.1111/j.1365-313X.2010.04181.x.

Manaia, J.P., Manaia, A.T., Rodriges, L., 2019. Industrial hemp fibers: an overview. Fibers 7, 106. https://doi.org/10.3390/fib7120106.

Mangeot-Peter, L., Legay, S., Hausman, J.F., Esposito, S., Guerriero, G., 2016. Identification of reference genes for RT-qPCR data normalization in *Cannabis sativa* stem tissues. Int. J. Mol. Sci. 17, 1556. https://doi.org/10.3390/ijms17091556.

Mokshina, N., Chernova, T., Galinousky, D., Gorshkov, O., Gorshkova, T., 2018. Key stages of fiber development as determinants of bast fiber yield and quality. Fibers 6, 20. https://doi.org/10.3390/fib6020020.

Nkongolo, K.K., Spiers, G., Beckett, P., Narendrula-Kotha, R., 2022. Effects of phytoremediation on microbial biomass, composition, and function in a sulphide-rich tailing from a metal-contaminated region. Front. Environ. Sci. 10, 908633. https://doi.org/10.3389/fenvs.2022.908633.

Parrotta, L., Guerriero, G., Sergeant, K., Cai, G., Hausman, J.F., 2015. Target or barrier? The cell wall of early- and later-diverging plants vs cadmium toxicity: differences in the response mechanisms. Front. Plant Sci. 6, 133. https://doi.org/10.3389/fpls.2015.00133.

Sharma, A., Patni, B., Shankhdhar, D., Shankhdhar, S.C., 2013. Zinc – an indispensable micronutrient. Physiol. Mol. Biol. Plants 19, 11–20. https://doi.org/10.1007/s12298-012-0139-1.

Siemianowski, O., Rongpipi, S., Del Mundo, J.T., Freychet, G., Zhernenkov, M., Gomez, E.D., Gomez, E.W., Anderson, C.T., 2024. Flexible pectin nanopatterning drives cell wall organization in plants. JACS Au 4, 177–188. https://doi.org/10.1021/jacsau.3c00616.

Šípošová, K., Labancová, E., Hačkuličová, D., Kollárová, K., Vivodová, Z., 2023. The changes in the maize root cell walls after exogenous application of auxin in the presence of cadmium. Environ. Sci. Pollut. Res. 30, 87102–87117. https://doi.org/10.1007/s11356-023-28029-3.

Tan, H.W., Pang, Y.L., Lim, S., Chong, W.C., 2023. A state-of-the-art of phytoremediation approach for sustainable management of heavy metals recovery. Environ. Technol. Innov. 30, 103043. https://doi.org/10.1016/j.eti.2023.103043.

Tolivia, D., Tolivia, J., 1987. Fasga: a new polychromatic method for simultaneous and differential staining of plant tissues. J. Microsc. 148, 113–117. https://doi.org/10.1111/j.1365-2818.1987.tb02859.x.

Vasilou, C., Tsiropoulos, N.G., Golia, E.E., 2024. Phytoremediation & valorization of Cu-contaminated soils through *Cannabis sativa* (L.) cultivation: a smart way to produce cannabidiol (CBD) in Mediterranean soils. Waste Biomass Valorization 15, 1711–1724. https://doi.org/10.1007/s12649-023-02388-x.

Wakabayashi, K., Soga, K., Hoson, T., Masuda, H., 2023. The modification of cell wall properties is involved in the growth inhibition of rice coleoptiles induced by lead stress. Life 13, 471. https://doi.org/10.3390/life13020471 (Basel).

Wang, R., Sang, P., Guo, Y., Jin, P., Cheng, Y., Yu, H., Xie, Y., Yao, W., Qian, H., 2023. Cadmium in food: source, distribution and removal. Food Chem. 405, 134666. https://doi.org/10.1016/j.foodchem.2022.134666.

Zhu, Y., Gu, H., Li, H., Lam, S.S., Verma, M., Ng, H.S., Sonne, C., Liew, R.K., Peng, W., 2024. Phytoremediation of contaminants in urban soils: a review. Environ. Chem. Lett. 22, 355–371.

Zhu, Q., Ji, J., Tang, C., Wang, C., Sun, H., 2023. Bioavailability assessment of heavy metals and organic pollutant in water and soil using DGT: a review. Applied Sci. 13, 9760.